

# Strong Coupling Corrections to the Ginzburg-Landau Theory of Superfluid $^3\text{He}$

H. Choi, J.P. Davis, J. Pollanen, T.M. Haard and W.P. Halperin

*Department of Physics and Astronomy,  
Northwestern University, Evanston, Illinois 60208*

(Dated: Version February 9, 2022)

In the Ginzburg-Landau theory of superfluid  $^3\text{He}$ , the free energy is expressed as an expansion of invariants of a complex order parameter. Strong coupling effects, which increase with increasing pressure, are embodied in the set of coefficients of these order parameter invariants<sup>1,2</sup>. Experiments can be used to determine four independent combinations of the coefficients of the five fourth order invariants. This leaves the phenomenological description of the thermodynamics near  $T_c$  incomplete. Theoretical understanding of these coefficients is also quite limited. We analyze our measurements of the magnetic susceptibility and the NMR frequency shift in the  $B$ -phase which refine the four experimental inputs to the phenomenological theory. We propose a model based on existing experiments, combined with calculations by Sauls and Serene<sup>3</sup> of the pressure dependence of these coefficients, in order to determine all five fourth order terms. This model leads us to a better understanding of the thermodynamics of superfluid  $^3\text{He}$  in its various states. We discuss the surface tension of bulk superfluid  $^3\text{He}$  and predictions for novel states of the superfluid such as those that are stabilized by elastic scattering of quasiparticles from a highly porous silica aerogel.

## I. INTRODUCTION

The Ginzburg-Landau (GL) formulation gives a phenomenological representation of the free energy of superfluid  $^3\text{He}$  as an expansion in terms of the order parameter<sup>1,2,3</sup>. The expansion coefficients specify the stability of various  $p$ -wave states and their thermodynamics near  $T_c$ . These coefficients are well-defined theoretically for the weak coupling case. However,  $^3\text{He}$  is not a weak coupling superfluid as is clear from its phase diagram where there is a region of  $A$ -phase at high pressures. This is in contrast to the weak coupling limit for which the  $B$ -phase is always stable. The strong coupling correction to the pair interaction is responsible for the  $A$ -phase, an effect of spin and density fluctuations proportional to  $T_c/T_F$ <sup>4</sup>. Calculations<sup>3</sup> cannot account quantitatively for the strong coupling corrections and so the coefficients must be determined empirically. Five of these parameters are coefficients of the fourth order invariants of the order parameter in the GL free energy. These are called the  $\beta$ -parameters,  $\beta_i$ 's where  $i = 1, \dots, 5$ . Unfortunately, there are not enough independent sets of experiments to determine all the parameters and so the phenomenological description of superfluid  $^3\text{He}$  is under determined. This hampers our ability to predict stability for novel superfluid  $p$ -wave states, such as those that might be favored by elastic scattering from high porosity silica aerogel.

In this paper, we present four combinations of  $\beta_i$ 's which we determine from measurements and we describe a model which resolves the ambiguity in identifying all five of them independently. The coefficient of a field dependent term in GL theory,  $g_z$ , plays an important role in determining more accurate combinations of the  $\beta_i$  than have been previously reported. Our NMR measurements of the susceptibility<sup>5</sup> show that  $g_z$  is close to its weak coupling value at all pressures. This allows us to interpret our high resolution measurements of the NMR

frequency shift in the  $B$ -phase<sup>6,7</sup> and to obtain accurate  $\beta$ -parameter combinations.

Our model for determining the five  $\beta_i$ 's is motivated by the calculations of Sauls and Serene<sup>3</sup>. We note that the calculations, although only qualitatively consistent with the existing experiments, nonetheless can accurately account for their pressure dependence. Furthermore, we note that the calculations indicate that one of the  $\beta$ -parameters,  $\beta_1$ , is close to its weak coupling value at all pressures. Motivated by these observations and the fact that the experimentally known combinations of the  $\beta_i$ 's approach their weak coupling values at zero pressure to within 5%, we make the following two assumptions: First, the  $\beta$ -parameters are, on average, close to their weak coupling values at zero pressure and we use this criterion to select  $\beta_1$  at zero pressure. Second, we take their pressure dependences from the theory which seems to accurately represent this aspect of the known  $\beta$ -parameter combinations. These assumptions are sufficient to constitute a model to determine the full suite of  $\beta$ -parameters. With this information we can calculate the surface tension between  $A$ - and  $B$ -phases in bulk superfluid  $^3\text{He}$  and compare with experiment. We can also calculate the stability of the axi-planar state in bulk superfluid  $^3\text{He}$  as a function of pressure and we can evaluate predictions for anisotropic  $p$ -wave states that are robust in the presence of elastic scattering from silica aerogel.

## II. GL THEORY FOR $^3\text{HE}$

A phenomenological macroscopic description of phase transitions is given by the GL theory, in which the free energy is expressed as an expansion of the order parameter. In the case of superfluid  $^3\text{He}$ , the order parameter<sup>2,8</sup>,  $A$ , is a complex  $3 \times 3$  matrix and the free energy of the

system can be expressed as,

$$\begin{aligned}
F = & -\alpha \text{Tr}(AA^\dagger) + g_z H_\mu (AA^\dagger)_{\mu\nu} H_\nu + \beta_1 |\text{Tr}(AA^T)|^2 \\
& + \beta_2 [\text{Tr}(AA^\dagger)]^2 + \beta_3 \text{Tr}(AA^T (AA^T)^*) \\
& + \beta_4 \text{Tr}((AA^\dagger)^2) + \beta_5 \text{Tr}(AA^\dagger (AA^\dagger)^*). \quad (1)
\end{aligned}$$

Here the dipole energy term is neglected. The magnetic field components are  $H_\mu$ , and  $A^\dagger$  and  $A^T$  are the Hermitian conjugate and transpose of  $A$ . The structure of the order parameter admits five fourth order invariants each of which has a corresponding coefficient,  $\beta_i$ . At the second order thermodynamic transition to superfluidity,  $T_c$ , all  $p$ -wave superfluid states are equally probable, but their stability below  $T_c$  depends on the  $\beta_i$ . In the weak-coupling limit the free energy coefficients are,

$$\alpha = \frac{N(0)}{3} \left( \frac{T}{T_c} - 1 \right), \quad (2)$$

$$\frac{\beta_i}{\beta_0} = (-1, 2, 2, 2, -2), i = 1, \dots, 5, \quad (3)$$

$$\beta_0 = \frac{7\zeta(3)}{120\pi^2} \frac{N(0)}{(k_B T_c)^2}, \quad (4)$$

$$g_z = \frac{7\zeta(3)}{48\pi^2} N(0) \left( \frac{\gamma_0 \hbar}{(1+F_0^a) k_B T_c} \right)^2, \quad (5)$$

where the normal density of states at the Fermi energy is  $N(0)$ , the gyromagnetic ratio for  $^3\text{He}$  is  $\gamma_0$ ,  $k_B$  is the Boltzmann constant,  $F_0^a$  is a Fermi liquid parameter determined from the magnetization measurement<sup>8</sup> and  $\zeta(x)$  is the Riemann zeta function. However,  $^3\text{He}$  is not a weak coupling superfluid and strong coupling effects increase with pressure. The strong coupling corrections for  $\alpha$  are negligible<sup>3</sup> but they have a significant effect on the  $\beta_i$ 's, and might also contribute to  $g_z$ . Calculations of strong coupling corrections have been performed for model potentials<sup>3,9</sup>; those of Sauls and Serene<sup>3</sup> being the most complete and the ones we will refer to in this work.

### III. EXPERIMENTS

There are seven free energy coefficients which must be determined from experiment. The difficulty lies in the fact that there is insufficient experimental input to constrain this phenomenological description of superfluid  $^3\text{He}$ . Among the seven coefficients,  $\alpha$  and  $g_z$  are determined without ambiguity. The measurements of the specific heat in the normal state,  $C_N$  and the transition temperature<sup>10</sup>,  $T_c$ , give us  $\alpha$ . The slope of the  $^3\text{He}$ - $B$  magnetization<sup>5</sup> extrapolated to  $T_c$ ,  $dM_B/dT|_{T_c}$ , and the specific heat jump<sup>10</sup> of  $^3\text{He}$ - $B$ ,  $\Delta C_B/C_N$ , are required for  $g_z$ , for which we have new results presented in this section. For the remaining five  $\beta_i$ 's, there are only four independent sets of experiments so that only four combinations of  $\beta_i$ 's can be found in the form of sums. These are  $\beta_{345}$ ,  $\beta_{12}$ ,  $\beta_{245}$ , and  $\beta_5$ , where we use the Mermin-Stare convention,  $\beta_{ij} = \beta_i + \beta_j$ .

First, we will describe the relevant experiments and the logic for determining these combinations of the  $\beta_i$ 's.

A).  $\beta_{345}$  requires measurements of the  $^3\text{He}$ - $B$  transverse NMR  $g$ -shift<sup>6,7</sup>,  $g$ , which must be combined with the slope of the  $B$ -phase longitudinal NMR resonance frequency<sup>7,11,12</sup>,  $\nu_{B||}^2/(1-t)$ , in the limit approaching  $T_c$  as well as with measurements of  $\Delta C_B/C_N$ <sup>10</sup> where  $t = T/T_c$ . In order to have the value of the  $g$ -shift at  $T_c$  it is helpful to observe that the  $B$ -phase susceptibility and the  $g$ -shift are linearly related, facilitating an extrapolation to  $T_c$ . The  $B$ -phase heat capacity jump is measured only below the polycritical point (PCP). However, measurement of the specific heat in the  $A$ -phase along with measurements of the latent heat at the  $A$ - to  $B$ -transition allows a thermodynamic calculation<sup>10</sup> of the specific heat jump for the  $B$ -phase at pressures above the PCP. Consequently,  $\Delta C_B/C_N$  is experimentally determined at all pressures.

B). From the specific heat jump,  $\Delta C_B/C_N$  and the values for  $\beta_{345}$  obtained above we can directly determine  $\beta_{12}$ .

C). From the specific heat jump,  $\Delta C_A/C_N$  we can directly determine  $\beta_{245}$ , but only for pressures greater than the PCP where this jump can be measured. Below the PCP  $\beta_{245}$  is found from the quadratic magnetic field suppression of the first order  $^3\text{He}$   $A$ - to  $B$ -transition<sup>13</sup>,  $g(\beta)$ , along with the values of  $\beta_{12}$  and  $\beta_{345}$  that have been obtained above in A) and B).

D). Finally, we can fix  $\beta_5$  uniquely by the asymmetry ratio,  $r$ , of the linear field dependent splitting of the  $A_1$  to  $A_2$  transitions<sup>14</sup> in high magnetic field combined with  $\beta_{245}$ .

In summary, four independent combinations of experiments gives us four constraints on the  $\beta_i$ 's, which is insufficient to identify all five of them. In principle, measurement of the surface tension at the  $^3\text{He}$   $A$ - $B$  interface could provide us with a fifth independent combination<sup>15,16,17</sup> of  $\beta_i$ 's. However, the surface tension vanishes near  $T_c$  due to the degeneracy of the free energy at  $T_c$  of  $A$ - and  $B$ -phases. For this reason it is not possible to obtain sufficiently high resolution measurements of the surface tension to provide useful characterization of strong coupling effects in the Ginzburg-Landau limit. In the following, we will discuss in more detail the experimental determination of strong coupling and its effects on the  $\beta_i$ 's.

The coefficient for the field coupling term,  $g_z$ , is determined by measuring the slope of the magnetization of  $^3\text{He}$ - $B$  in the limit approaching  $T_c$ ,

$$\hat{g}_z \equiv \frac{g_z}{g_z^{\text{wc}}} = \frac{\frac{dm}{dt}}{\left(\frac{dm}{dt}\right)^{\text{wc}}} \frac{\Delta C_B^{\text{wc}}}{\Delta C_B}, \quad (6)$$

where  $m = M_B/M_N$  and  $M_N$  is the normal state magnetization. The superscript wc, which we use here and in the following, indicates the weak coupling limit.

Magnetization measurements of superfluid  $^3\text{He}$  have been of great interest since its discovery. Two different techniques - NMR based dynamic measurements<sup>5,18,19,20,21</sup> and SQUID based static

$P$ bar	$g$ -shift $\times 10^6$	$\frac{d\nu_{B\parallel}^2}{dt}$ $10^{10} \text{ Hz}^2$	$g(\beta)$	$\frac{\Delta C_B}{C_N}$	$\frac{\Delta C_A}{C_N}$	$-\frac{(\frac{dT}{dH})_{A1}}{(\frac{dT}{dH})_{A2}}$	$\frac{\beta_{345}}{\beta_0}$	$\frac{\beta_{12}}{\beta_0}$	$\frac{\beta_{245}}{\beta_0}$	$\frac{\beta_5}{\beta_0}$
w.c.			1	1.426	1.188	1	2	1	2	-2
0	7.31	1.50	1.61	1.46	1.25	0.97	2.11	0.92	1.90	-1.84
1	7.71	1.78	1.72	1.50	1.29	0.99	1.86	0.97	1.84	-1.82
2	8.10	2.06	1.84	1.53	1.33	1.02	1.68	0.99	1.78	-1.81
3	8.48	2.34	1.96	1.56	1.37	1.04	1.56	1.01	1.74	-1.81
4	8.85	2.62	2.07	1.58	1.40	1.07	1.47	1.01	1.70	-1.81
5	9.20	2.90	2.20	1.61	1.43	1.09	1.41	1.01	1.66	-1.81
6	9.55	3.18	2.37	1.63	1.46	1.12	1.36	1.01	1.63	-1.82
7	9.89	3.46	2.57	1.65	1.49	1.14	1.32	1.00	1.60	-1.82
8	10.22	3.74	2.80	1.67	1.51	1.16	1.29	1.00	1.57	-1.83
9	10.54	4.02	3.06	1.68	1.54	1.19	1.26	0.99	1.55	-1.84
10	10.86	4.30	3.34	1.70	1.56	1.21	1.24	0.98	1.52	-1.85
11	11.17	4.58	3.66	1.71	1.58	1.24	1.23	0.98	1.50	-1.86
12	11.47	4.86	4.03	1.73	1.61	1.26	1.21	0.97	1.48	-1.87
13	11.77	5.14	4.51	1.74	1.63	1.29	1.20	0.96	1.46	-1.88
14	12.06	5.42	5.20	1.75	1.66	1.31	1.19	0.96	1.44	-1.89
15	12.36	5.70	6.21	1.77	1.68	1.34	1.18	0.95	1.41	-1.89
16	12.64	5.98	7.70	1.78	1.71	1.36	1.17	0.95	1.39	-1.90
17	12.93	6.26	9.81	1.79	1.73	1.39	1.15	0.94	1.37	-1.90
18	13.22	6.54	12.71	1.80	1.76	1.41	1.14	0.94	1.35	-1.91
19	13.50	6.82	16.53	1.81	1.78	1.44	1.13	0.93	1.34	-1.92
20	13.79	7.10	21.30	1.82	1.80	1.46	1.12	0.93	1.32	-1.93
21	14.08	7.38		1.83	1.83	1.49	1.10	0.93	1.30	-1.93
22	14.36	7.66		1.84	1.85	1.51	1.09	0.92	1.28	-1.94
23	14.65	7.94		1.86	1.87	1.54	1.08	0.92	1.27	-1.95
24	14.95	8.22		1.87	1.90	1.56	1.06	0.92	1.25	-1.96
25	15.25	8.50		1.88	1.92	1.58	1.05	0.92	1.24	-1.97
26	15.55	8.78		1.89	1.94	1.61	1.03	0.91	1.23	-1.97
27	15.85	9.06		1.90	1.96	1.63	1.02	0.91	1.21	-1.98
28	16.17	9.34		1.91	1.98	1.66	1.00	0.91	1.20	-1.99
29	16.49	9.62		1.92	2.00	1.68	0.99	0.91	1.19	-2.00
30	16.81	9.90		1.93	2.02	1.71	0.97	0.91	1.18	-2.01
31					2.04	1.73			1.16	-2.02
32					2.07	1.76			1.15	-2.02
33					2.09	1.78			1.14	-2.03
34					2.12	1.81			1.12	-2.03

TABLE I: Ginzburg-Landau  $\beta$ -parameters and the experimental quantities from which they are derived. The NMR  $B$ -phase  $g$ -shift is a fit to data from Kycia<sup>7</sup> given by Haard<sup>5</sup>. The NMR  $B$ -phase longitudinal resonance was measured by Rand<sup>11,12</sup> for which a smoothed fit is given by Haard<sup>5</sup>. The coefficient of quadratic magnetic field suppression of the  $B$ -phase was measured by Tang *et al.*<sup>13</sup>. The  $B$ -phase heat capacity jump was taken from Greywall<sup>10</sup> and the asymmetry ratio of the linear field dependent splitting of the  $A_1$  to  $A_2$  transitions was reported by Israelson *et al.*<sup>14</sup>. Extension of the measurements of the  $A$ -phase heat capacity jump to pressures lower than the PCP requires a calculation based on the measured quadratic suppression of the  $A$ - to  $B$ -transition as described in the text.

measurements<sup>22,23,24,25</sup> - have been performed over the past thirty years. Historically, there has been a discrepancy between these two techniques<sup>26,27</sup> the origin of which has not been established. Nonetheless, more recent experiments<sup>5,28</sup> bring the results closer together. Haard measured the magnetization using high resolution NMR<sup>5</sup>. A careful analysis of this and other measurements<sup>28,29</sup> reveals that the discrepancy appears to be negligible near the transition temperature  $T_c$ . Using Eq. 6, Haard<sup>5</sup> determined  $g_z$  from NMR and found the results presented in Fig. 1, where  $g_z$  is close to its weak coupling value, i.e.  $\hat{g}_z = 1$ . From Haard's measurement, the deviation from weak coupling appears to grow slightly with pressure. From analysis<sup>5</sup> of the more accurate work of Scholz *et al.*<sup>21,29</sup> it appears that

$g_z$  is pressure independent. The difference between the data sets is likely due to the wider range of extrapolation in the  $B$ -phase toward  $T_c$  that is required to determine  $g_z$  at elevated fields in the case for Haard's measurement. Hahn *et al.*<sup>28</sup> came to the same conclusion,  $\hat{g}_z = 1$ , based on their SQUID measurements, and so we will take  $g_z$  to have its weak coupling value at all pressures. Having established  $g_z$ ,  $\beta_{345}$  can be calculated from the NMR  $g$ -shift<sup>5,6,7,30</sup> of the transverse NMR frequency in  $^3\text{He-}B$  which has the following relationship<sup>31</sup> with  $\hat{g}_z$  and  $\beta_{345}$ :

$$\frac{\beta_{345}}{\hat{g}_z} = \frac{\beta_{345}^{wc}}{(1 + F_0^a)^2} \left( \frac{C_N}{\Delta C_B} \right) \frac{\nu_{B\parallel}^2}{1 - t} \left( \frac{\hbar}{2\pi k_B T_c} \right)^2 \frac{1}{g}. \quad (7)$$

In earlier reports<sup>6</sup> of the  $g$ -shift, the analysis to ob-

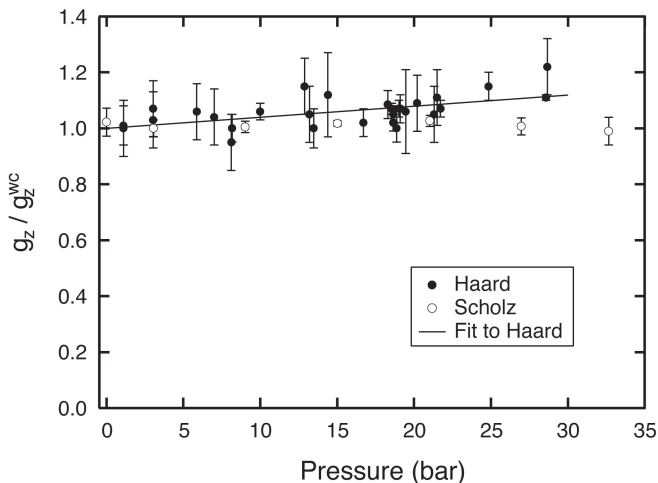


FIG. 1:  $\hat{g}_z$  obtained from magnetization measurements by NMR. Closed circles are the measurements by Haard<sup>5</sup> and open circles by Scholz<sup>21,29</sup>. The results from both measurements are consistent and give approximately unity for  $\hat{g}_z$

tain  $\beta_{345}$  estimated  $g_z$  incorrectly. The values in Table I for the  $g$ -shift and the  $B$ -phase longitudinal resonance frequency are smoothed values<sup>5</sup> from a large number of experiments<sup>7</sup>, significantly more than what was originally reported by Kycia *et al.*<sup>6</sup>. Greywall<sup>10</sup> has measured the specific heat of  ${}^3\text{He}$ - $A$  and  $B$ . The specific heat jump at  $T_c$ , for these two phases, is related to  $\beta_A$  and  $\beta_B$  through:

$$\Delta C_A = \frac{\alpha'^2}{2\beta_A}, \beta_A \equiv \beta_{245} \quad (8)$$

$$\Delta C_B = \frac{\alpha'^2}{2\beta_B}, \beta_B \equiv \beta_{12} + \frac{1}{3}\beta_{345}, \quad (9)$$

where  $\alpha' \equiv d\alpha/dT$ . At pressures less than the PCP, the magnetic suppression<sup>13</sup>,  $g(\beta)$ , of the  $AB$  transition temperature,  $T_{AB}$ , is used to obtain  $\beta_{245}$  through:

$$g(\beta) = -\frac{\sqrt{1 + (\beta_B/\beta_A - 1)(1 + \frac{2}{1 - \beta_{12}/\beta_B})} + 1}{\beta_B/\beta_A - 1}. \quad (10)$$

Here  $g(\beta)$  is defined by,

$$1 - \frac{T_{AB}}{T_c} \equiv g(\beta) \left(\frac{B}{B_0}\right)^2 + \mathcal{O}\left(\left(\frac{B}{B_0}\right)^4\right), \quad (11)$$

where  $B$  is the applied magnetic field and  $B_0^2 = N(0)/6g_z$ . Finally,  $\beta_5$  can be determined by measuring the asymmetry ratio<sup>14</sup> of the  $A_1$ - $A_2$  splitting,  $r$ ,

$$r \equiv \frac{T_{A1} - T_c}{T_c - T_{A2}} = -\frac{\beta_5}{\beta_{245}}. \quad (12)$$

The four experimentally determined  $\beta$ -coefficient combinations, along with the measurements used to obtain them, are tabulated from 0 to 34 bar in Table I.

## IV. MODEL FOR DETERMINING $\beta$ 'S

As stated earlier, we impose two assumptions to eliminate ambiguity associated with sorting out all five  $\beta_i$ 's from the four known combinations of  $\beta_i$ 's determined from the experiments described in the previous section. The assumptions are: 1) the pressure dependence of  $\beta_1$  calculated by Sauls and Serene<sup>3</sup> is valid. 2) At zero pressure, all five  $\beta_i$ 's approach their weak coupling values, on the average. The consequences of these assumptions will be discussed in the following subsections.

### A. Comparison with the Calculation

Sauls and Serene<sup>3</sup> developed a potential scattering model to find the strong coupling corrections to the  $\beta$ -coefficients in the pressure range of 12 to 34.4 bar. Since we do not have five experimentally determined  $\beta$ -coefficients with which to directly compare to the theory, we construct from the calculation those four combinations of  $\beta$ -coefficients,  $\beta_{345}$ ,  $\beta_{12}$ ,  $\beta_{245}$ , and  $\beta_5$  that are experimentally accessible and compare these with the measurements in Fig. 2. First, we note that the experimental results suggest that superfluid  ${}^3\text{He}$  is predominantly weak coupling at zero pressure. Secondly, the pressure dependence of each combination shows remarkable agreement between experiment and theory for  $P > 12$  bar, the range where the calculations were performed. It is also apparent that the calculation of the absolute values of the  $\beta_i$ 's is less reliable than their pressure dependence. Finally we note that, in the calculation, the smallest strong coupling correction among the  $\beta_i$ 's is for  $\beta_1$ . Guided by this information, we will assume that the pressure dependence of

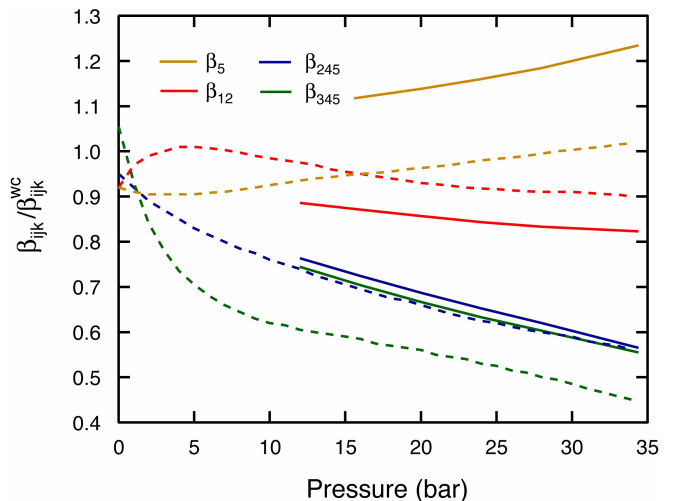


FIG. 2: Comparison of four known  $\beta$ -combinations from the experiments (dashed lines) and Sauls and Serene's calculation<sup>3</sup> (solid lines). The pressure dependences are in good agreement but the absolute values are not as close.

$\beta_1(P)$  can be taken from the Sauls and Serene calculation and then we need only determine  $\beta_1(0)$ .

### B. Zero Pressure Values of the $\beta_i$ 's

The pressure dependence of the  $\beta_i$ 's is insufficient to resolve the ambiguity associated with the  $\beta$  coefficient combinations. Five independent values of  $\beta_i$ 's at a given pressure are required along with the pressure dependence for  $\beta_1$ . The calculations indicate that strong coupling corrections are smallest for  $\beta_1(P)$  and from experiment we see that the measurable combinations deviate from their weak coupling values by less than 5% at zero pressure. On this basis one possibility would be to simply choose  $\beta_1(0)/\beta_1^{wc} = 1$ , *i.e.* to be weak coupling. Another possibility, the more democratic one, is to choose  $\beta_1(0)$  as a variational parameter and minimize the mean square deviations of all  $\beta$ -parameters from their weak coupling values at zero pressure subject to the constraints imposed by the four different combinations that have been determined experimentally. For the latter method we find  $\beta_1(0)/\beta_1^{wc} = 0.97$  which is essentially equivalent to the first choice. In the following we make the latter choice. We show this process explicitly in Fig. 3 where we calculate all of the  $\beta_i(0)$ 's as a function of  $\beta_1(0)$  subject to the four experimental constraints. It is clear that for  $\beta_1(0)$  near its weak coupling value, as emphasized by the circled region, all the others approach their weak coupling values at zero pressure as well. With this choice for  $\beta_1(0)$  and the pressure dependence of  $\beta_1$  taken from Sauls and Serene<sup>3</sup>,  $\beta_1(P)$  is now uniquely defined and all the other  $\beta_i$ 's can be determined. These  $\beta_i$ 's are tabulated in the first five columns of Table II.

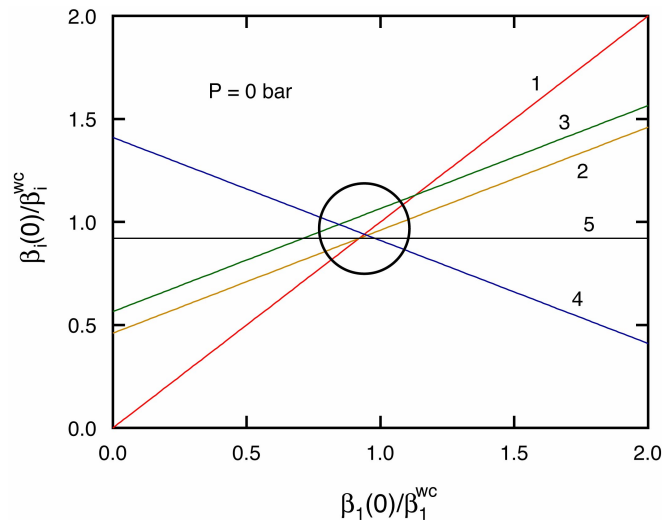


FIG. 3: Zero pressure values of the  $\beta_i$ 's parameterized by  $\beta_1(0)$ . The numbers on each line correspond to the subscript  $i$  of  $\beta_i$ . The  $\beta_i(0)$ 's clearly converge around  $\beta_i(0)/\beta_i^{wc} = 1$ , which is an indication that the  $\beta_i$ 's tend toward their weak-coupling values at low pressure.

## V. APPLICATIONS

### A. Surface Tension at the $A$ - $B$ Interface

With all the  $\beta_i$ 's now determined, one can calculate the surface tension between the  $A$ - and  $B$ -phases of superfluid  $^3\text{He}$ . According to Thuneberg<sup>15</sup>, the surface free energy of the  $A$ - $B$  interface is expressed as

$$f_{AB} = \frac{\xi(T)\alpha^2}{4\beta_2^{(0)}} \times \left[ \frac{I_1}{\sqrt{2\beta_2^{(0)}}} + \frac{I_2}{2} \left( \frac{4a^3}{\beta_2^{(0)}\beta_3^{(0)}(\beta_1^{(0)} + 3\beta_2^{(0)})} \right)^{\frac{1}{4}} \right] \quad (13)$$

where  $\xi(T)$  is the temperature dependent coherence length of  $^3\text{He}$ ,

$$I_1 = \begin{cases} \sqrt{a+c} + \frac{a}{\sqrt{c}} \ln \left( \frac{\sqrt{a+c} + \sqrt{c}}{\sqrt{a}} \right) & \text{if } c > 0 \\ \sqrt{a+c} + \frac{a}{\sqrt{-c}} \arcsin(\sqrt{-c/a}) & \text{if } c < 0, \end{cases} \quad (14)$$

$$I_2 \approx 1.89 - 1.98\sqrt{\kappa} - 0.31\kappa \text{ for } \kappa < 1/\sqrt{2}, \quad (15)$$

$$\kappa^2 = \frac{\beta_3^{(0)}(\beta_1^{(0)} + 3\beta_2^{(0)})}{4\beta_2^{(0)}\beta_{34}^{(0)}}. \quad (16)$$

Here  $a$  and  $c$  are defined as  $a = 2\beta_1 + \beta_3 - \beta_{45}$  and  $c = -(2\beta_1 + \beta_{345})$ . The  $\beta_i^{(0)}$ 's are any set of  $\beta_i$ 's that satisfy the condition for the surface energy to vanish,  $2\beta_1 + \beta_3 = 0, \beta_{45} = 0$ . Weak coupling values of  $\beta_i$ 's are a subset of the  $\beta_i^{(0)}$ 's, but the  $\beta_i^{(0)}$ 's need not be limited

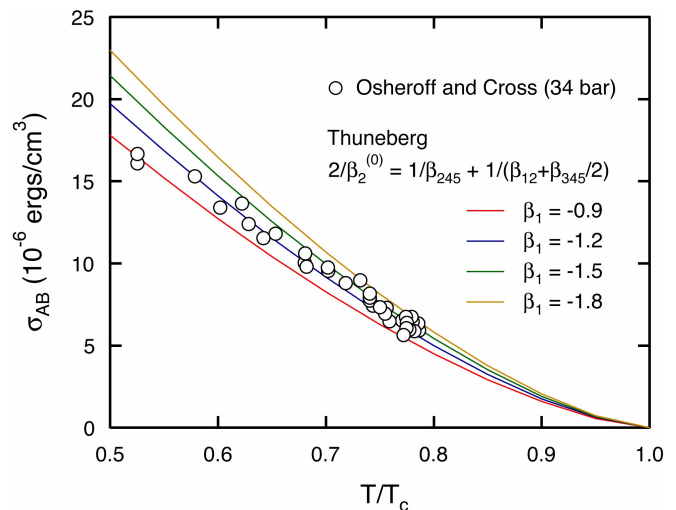


FIG. 4: Osheroff and Cross's measurements of surface tension<sup>16</sup> in comparison to the calculation by Thuneberg<sup>15</sup> for various  $\beta_1$  choices and  $2/\beta_2^{(0)} = 1/\beta_{245} + 1/(\beta_{12} + \beta_{345}/2)$ . The comparison of the two with the choice of  $\beta_1/\beta_1^{wc} \sim 1$  is consistent, but the measurement lacks the resolution to conclusively determine the value of  $\beta_1$ .

$P$ (bar)	Pure $^3\text{He}$					$^3\text{He}$ in 98% aerogel				
	$\frac{\beta_1}{\beta_0}$	$\frac{\beta_2}{\beta_0}$	$\frac{\beta_3}{\beta_0}$	$\frac{\beta_4}{\beta_0}$	$\frac{\beta_5}{\beta_0}$	$\frac{\beta_1^a}{\beta_0^a}$	$\frac{\beta_2^a}{\beta_0^a}$	$\frac{\beta_3^a}{\beta_0^a}$	$\frac{\beta_4^a}{\beta_0^a}$	$\frac{\beta_5^a}{\beta_0^a}$
w.c.	-1	2	2	2	-2	-1	2	2	2	-2
0	-0.97	1.89	2.10	1.85	-1.84					
1	-0.97	1.94	1.96	1.72	-1.82					
2	-0.97	1.96	1.86	1.63	-1.81					
3	-0.98	1.99	1.81	1.56	-1.81					
4	-0.98	1.99	1.76	1.52	-1.81					
5	-0.98	1.99	1.74	1.48	-1.81	-0.05	0.15	0.10	0.15	-0.15
6	-0.98	1.99	1.72	1.46	-1.82	-0.20	0.51	0.36	0.48	-0.50
7	-0.98	1.98	1.70	1.44	-1.82	-0.28	0.72	0.53	0.66	-0.70
8	-0.98	1.98	1.70	1.42	-1.83	-0.35	0.87	0.66	0.78	-0.84
9	-0.99	1.98	1.69	1.41	-1.84	-0.41	0.99	0.75	0.87	-0.95
10	-0.99	1.97	1.69	1.40	-1.85	-0.45	1.08	0.83	0.94	-1.05
11	-0.99	1.97	1.70	1.39	-1.86	-0.49	1.15	0.90	0.99	-1.12
12	-0.99	1.96	1.69	1.39	-1.87	-0.52	1.21	0.96	1.03	-1.17
13	-0.99	1.95	1.69	1.39	-1.88	-0.55	1.26	1.01	1.06	-1.22
14	-1.00	1.95	1.70	1.38	-1.89	-0.58	1.30	1.05	1.09	-1.27
15	-1.00	1.95	1.72	1.35	-1.89	-0.60	1.34	1.10	1.10	-1.32
16	-1.00	1.95	1.73	1.34	-1.90	-0.62	1.38	1.13	1.12	-1.35
17	-1.00	1.94	1.72	1.33	-1.90	-0.64	1.40	1.16	1.13	-1.38
18	-1.00	1.94	1.73	1.32	-1.91	-0.66	1.43	1.19	1.14	-1.41
19	-1.00	1.93	1.72	1.33	-1.92	-0.67	1.45	1.21	1.16	-1.43
20	-1.01	1.94	1.74	1.31	-1.93	-0.69	1.48	1.24	1.16	-1.47
21	-1.01	1.94	1.74	1.29	-1.93	-0.71	1.50	1.26	1.16	-1.49
22	-1.01	1.93	1.74	1.29	-1.94	-0.72	1.51	1.28	1.17	-1.51
23	-1.01	1.93	1.74	1.29	-1.95	-0.73	1.53	1.30	1.18	-1.53
24	-1.01	1.93	1.74	1.28	-1.96	-0.74	1.54	1.32	1.18	-1.54
25	-1.01	1.93	1.74	1.28	-1.97	-0.75	1.56	1.33	1.18	-1.58
26	-1.02	1.93	1.73	1.27	-1.97	-0.76	1.57	1.34	1.18	-1.60
27	-1.02	1.93	1.74	1.26	-1.98	-0.77	1.58	1.36	1.18	-1.61
28	-1.02	1.93	1.73	1.26	-1.99	-0.78	1.60	1.37	1.19	-1.62
29	-1.02	1.93	1.73	1.26	-2.00	-0.78	1.61	1.38	1.19	-1.63
30	-1.02	1.93	1.72	1.26	-2.01	-0.79	1.62	1.38	1.19	-1.67
31	-1.03	1.93	1.73	1.25	-2.02	-0.80	1.62	1.40	1.19	-1.68
32	-1.03	1.93	1.73	1.25	-2.02	-0.81	1.63	1.40	1.19	-1.68
33	-1.03	1.93	1.73	1.25	-2.03	-0.81	1.63	1.41	1.19	-1.69
34	-1.03	1.93	1.73	1.25	-2.03	-0.82	1.64	1.42	1.20	-1.70

TABLE II:  $\beta_i$ 's for bulk superfluid  $^3\text{He}$ , left side, and superfluid  $^3\text{He}$  in 98% porosity aerogel in the IISM with  $\lambda=150$  nm and  $\xi_a=40$  nm, right side.

to their weak coupling values. Thuneberg suggested two different values for  $\beta_2^{(0)}$ ,  $2/\beta_2^{(0)} = \beta_{245}^{-1} + (\beta_{12} + \beta_{345}/2)^{-1}$  and  $\beta_2^{(0)} = \beta_{12} + \beta_{345}/2$ , but kept the relative magnitude of the five  $\beta_i^{(0)}$ 's the same as for the weak-coupling case in his original work<sup>15</sup>. We examined these two choices of  $\beta_2^{(0)}$ .

From a number of different choices for the  $\beta_1$  including the values of the  $\beta_1$  chosen from Table I, the surface tension at the melting curve is calculated. The calculation with our choice of  $\beta_1$  and the measurements of Osheroff and Cross<sup>16</sup> are in good agreement. An example of the calculation with  $2/\beta_2^{(0)} = \beta_{245}^{-1} + (\beta_{12} + \beta_{345}/2)^{-1}$  is shown in Fig. 4. The calculation, however, has a number of limitations. One is that the calculation depends on the choice of  $\beta_2^{(0)}$  which is not uniquely defined. The other is that the experimental results do not have high enough resolution to determine the  $\beta_i$ 's independently.

## B. How Stable Is the Axial State?

A number of experiments performed to investigate the order parameter of  $^3\text{He}$ -A phase have confirmed that the A-phase is, in fact, the axial state. This confirmation could be further strengthened by studying the thermodynamic stability of the axial state over other possible equal spin pairing states, such as an axi-planar state; some concern has been raised in the past that an axial state and an axi-planar state may not be easily distinguishable due to their continuously related order parameter structures<sup>13,32</sup>. However, a certain combination of  $\beta$ -coefficients, namely  $\beta_{45}$  can be used to check the relative thermodynamic stability between the two states. If  $\beta_{45}$  is negative, the A-phase is the axial state and if  $\beta_{45}$  is positive, the A-phase would be the axi-planar state. By imposing  $\beta_{45} = 0$  as the fifth constraint in addition to the four known combinations of the  $\beta_i$ 's, a unique set of  $\beta_i$ 's is obtained which can be used to plot a phase diagram

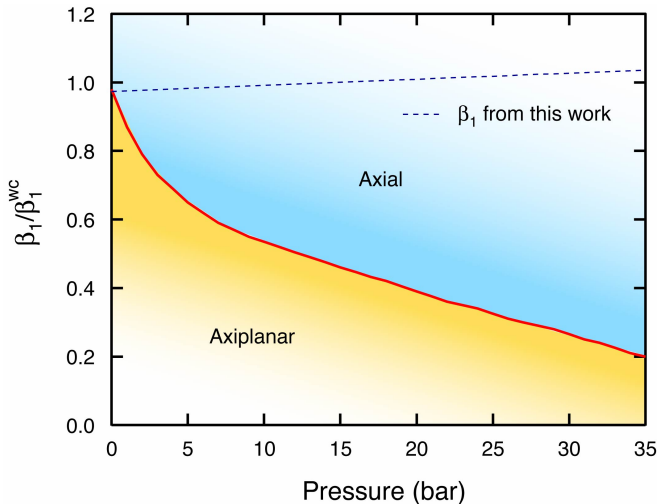


FIG. 5: Phase diagram for axial and axi-planar states with  $\beta_1$  as a parameter. The choice of  $\beta_1$  with our model (dashed line) places the  $A$ -phase in the region of the axial state.

for axial and axi-planar states with  $\beta_1$  as a parameter. This phase diagram is shown in Fig. 5. We compare our choice of  $\beta_1$  from Table I with the phase diagram and this value lies well within the axial state regime at high pressure as has been commonly believed and which a number of experiments independently confirm<sup>11,12,33</sup>. However, it should be noted that our choice of  $\beta_1$  indicates that there is a near degeneracy of the axial and axi-planar states at zero pressure and this might be interesting to investigate further.

### C. The Robust Phase in Aerogel

Full determination of all five  $\beta_i$ 's has important implications for superfluid  $^3\text{He}$  in aerogel. Within the context of scattering models we can calculate the appropriate modifications to the  $\beta_i$ 's and explore the predicted stability of various superfluid states. There are multiple different scattering models for  $^3\text{He}$  in aerogel, e.g., the homogeneous isotropic scattering model (HISM)<sup>34</sup> and inhomogeneous isotropic scattering models (IISM)<sup>34,35,36</sup>. We use the IISM of Sauls and Sharma<sup>36</sup>, a modification of the HISM of Thuneberg *et al.*<sup>34</sup>. The  $\beta_i$ 's in the IISM are modified through:

$$\begin{pmatrix} \beta_1^a \\ \beta_2^a \\ \beta_3^a \\ \beta_4^a \\ \beta_5^a \end{pmatrix} = \beta_0^a \begin{pmatrix} -1 \\ 2 \\ 2 \\ 2 \\ -2 \end{pmatrix} + b \begin{pmatrix} 0 \\ 1 \\ 0 \\ 1 \\ -1 \end{pmatrix} + \begin{pmatrix} \Delta\beta_1^{sc,a} \\ \Delta\beta_2^{sc,a} \\ \Delta\beta_3^{sc,a} \\ \Delta\beta_4^{sc,a} \\ \Delta\beta_5^{sc,a} \end{pmatrix}, \quad (17)$$

$$\beta_0^a = \frac{N(0)}{30(\pi k_B T_c)^2} \sum_{n=1} \frac{1}{(2n-1+x)^3}, \quad (18)$$

$$b = \frac{N(0)}{9(\pi k_B T_c)^2} \left( \sin^2 \delta_0 - \frac{1}{2} \right) \sum_{n=1} \frac{x}{(2n-1+x)^4}, \quad (19)$$

where  $x = \hat{x}/(1+\zeta_a^2/\hat{x})$ ,  $\zeta_a = \xi_a/\lambda$ ,  $\hat{x} = \hbar v_F/2\pi k_B T \lambda$ ,  $\xi_a$  is the strand-strand correlation length,  $\lambda$  is the transport mean free path for  $^3\text{He}$  quasiparticles, and  $\delta_0$  is the  $s$ -wave scattering phase shift.

With the five  $\beta_i$ 's for bulk superfluid given in Table II, we calculated the effects on the  $\beta_i$ 's of scattering from the aerogel strands. We distinguish these coefficients from bulk  $^3\text{He}$  with a superscript,  $\beta_i^a$ . We assumed unitary scattering,  $\delta_0 = \pi/2$  with  $\lambda = 150$  nm and  $\xi_a = 40$  nm. These parameters are typical of 98% porosity aerogels<sup>37</sup>. The effects of scattering in the weak coupling approximation are included in both  $\beta_0^a$  and  $b$ . In addition, the  $\beta_i^a$ 's will have a strong coupling component that will be modified by elastic scattering. We accommodate this by rescaling the  $\Delta\beta_i^{sc}$ 's with a factor  $T_{ca}/T_c$ , since strong coupling effects<sup>4</sup> are linear in  $T_c/T_F$ . The results of the calculation,  $\beta_i^a/\beta_0^a$ , are tabulated in the last five columns of Table II. For this choice of aerogel parameters the superfluid state is not stable below a pressure of 5 bar as reported by Matsumoto *et al.*<sup>38</sup>, and hence the table is blank below this pressure.

A direct consequence of the modification of  $\beta_i^a$ 's according to the scattering model is the enhancement of relative stability of the  $B$ -phase with respect to the  $A$ -phase for  $^3\text{He}$  in aerogel. For either the HISM or IISM, the isotropic state ( $B$ -phase) is found to be stable over the entire pressure range. However, superfluid  $^3\text{He}$  in aerogel has a metastable  $A$ -like phase that has been clearly observed<sup>39,40,41</sup> in various samples on cooling below  $T_c$ . Although the exact nature of this phase is still in question, it is known that the metastable phase is an equal-spin-pairing state<sup>42</sup>, similar to the bulk  $A$ -phase, hence it is referred to as an  $A$ -like phase. However, lack of understanding of the orbital part of the order parameter makes the identity of the state less clear. Furthermore, the question of stability of any equal-spin-pairing state with respect to the aerogel  $B$ -phase relies on an understanding of the appropriate  $\beta$ -parameters for which we have no direct independent information. Volovik<sup>43</sup> has argued that the axial state in the presence of quenched anisotropic disorder cannot exist as a spatially homogeneous superfluid owing to arguments from Imry and Ma<sup>44</sup>. If the metastable phase is in fact the axial state, the order parameter would not have long range orientational order, a state which Volovik has called a superfluid glass. With a different approach, Fomin<sup>45</sup> has argued that there are other  $p$ -wave pairing states which are also equal-spin-pairing but do not suffer from the same difficulty, and that these might be candidates for the metastable aerogel phase. Such phases would be robust in the presence of anisotropic scattering, meaning that  $A_{\mu i} A_{\mu j}^* + A_{\mu j} A_{\mu i}^* \propto \delta_{ij}$  where  $\delta_{ij}$  is the Kronecker delta.<sup>45</sup> NMR experiments have been performed on  $^3\text{He}$  in 97.5% aerogel which support the view that

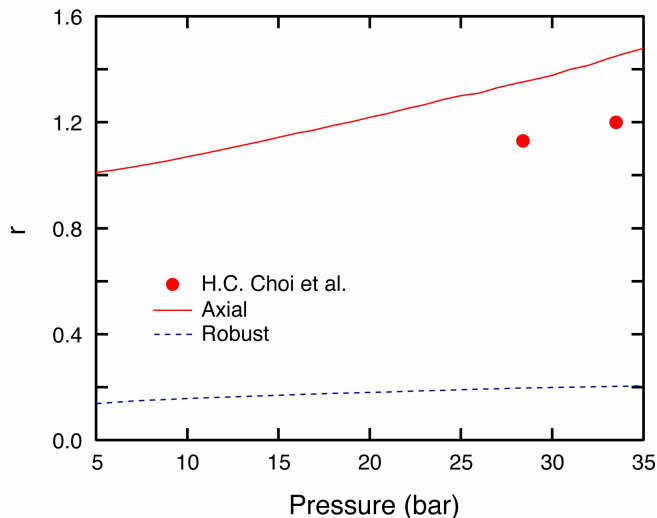


FIG. 6: The asymmetry ratio,  $r$ , for the  $A_1 - A_2$  splitting was calculated for the axial state (solid red line) and the robust phase (dashed line) in aerogel, where we used the IISM of Sauls and Sharma<sup>36</sup> with a transport mean free path for  $^3\text{He}$  quasiparticles  $\lambda = 150$  nm and strand-strand correlation length  $\xi_a = 40$  nm, which match well to phase diagram measurements on the same sample by Gervais *et al.*<sup>40</sup>. The measurements of H.C. Choi *et al.*<sup>48</sup> (closed circles) are more consistent with the  $A$ -like phase of aerogel  $^3\text{He}$  being the axial state than the robust state.

the metastable  $A$ -like phase is in fact a robust state<sup>46</sup>, but other measurements<sup>47,48,49</sup> appear to be inconsistent with this interpretation. The free energy for the robust state<sup>45</sup> can be expressed as,

$$F_R = -\alpha^2/4\beta_R, \quad (20)$$

where,

$$\beta_R = (\beta_{13} + 9\beta_2 + 5\beta_{45})/9. \quad (21)$$

Thermodynamic properties of the robust state have not been predicted because it involves all five  $\beta_i$ 's beyond the four combinations known to us so far. However, the determination of  $\beta_i$ 's from our model allows us to investigate the properties of the robust state. First, we calculate the asymmetry ratio of the  $A_1$ - $A_2$  splitting in aerogel. For the  $A$ -phase this ratio is expressed in terms of the  $\beta_i$ 's given by Eq. 12. In the case of the robust state the ratio  $r_R$  is given by<sup>45,48</sup>,

$$r_R = \frac{\beta_{15}}{\beta_{13} + 9\beta_2 + 5\beta_{45}}. \quad (22)$$

With the values of the  $\beta_i$ 's from Table II, the asymmetry ratio  $r_R$  is found to be  $\sim 0.2$ , considerably smaller than what has been found experimentally<sup>48</sup>,  $r_R \gtrsim 1.0$ . These results are compared in Fig. 6.

Second, we calculate the relative stability of the robust state with respect to the  $B$ -phase over the pressure range from zero to 34 bar with  $\beta_1$  for bulk  $^3\text{He}$  as a parameter subject to the constraints of the four experimentally

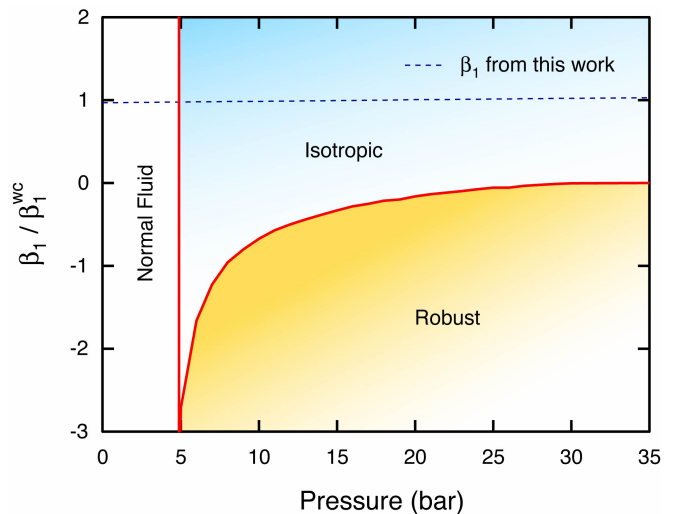


FIG. 7: Phase diagram for the isotropic phase and the robust phase for  $^3\text{He}$  in 98 % porosity aerogel with  $\beta_1$  (bulk) as a parameter. Our choice of  $\beta_1$  (dashed line) makes the isotropic phase more stable than the robust phase.

known combinations of the  $\beta$ 's given in Table I. These results are shown in Fig. 7. For the robust state of  $^3\text{He}$  in aerogel to be stable,  $\beta_1$  would have to be significantly different from the value derived from our model, assuming the form of the free energy in Eq. 1.

## VI. CONCLUSIONS

We have investigated the experimental basis for determining strong coupling as a function of pressure for superfluid  $^3\text{He}$  based on analysis of our NMR data. Given the limitation that we have only four experimentally identifiable  $\beta$ -coefficient combinations, we developed a phenomenological model with two assumptions: 1) that superfluid  $^3\text{He}$  is predominantly weak coupling at low pressure and 2) that the pressure dependence of  $\beta_1$  can be taken from Sauls and Serene's calculation. This model provides us with all five  $\beta$ -coefficients. Using this model we calculated the surface free energy at the  $A$ - $B$  interface and compared with experiment. Although the measurement does not have high enough resolution to validate our model, it is not in disagreement. The model is also consistent with the general consensus that the so-called  $A$ -phase is the axial phase rather than the axi-planar phase. We used our values of the  $\beta_i$ 's to calculate the corresponding strong coupling effects for superfluid  $^3\text{He}$  in aerogel. We find that the  $B$ -phase is stable at all pressures. We compared the relative stability of the robust state proposed by Fomin with that of the  $B$ -phase. The robust state is unstable relative to either the isotropic  $B$ -like phase or the axial state. Furthermore, the asymmetry ratio,  $r_R$ , of the  $A_1$ - $A_2$  splitting for superfluid  $^3\text{He}$  in aerogel was calculated for the robust state and



it was found to be significantly smaller than the experimental values. Our interpretation is that the  $A$ -like aerogel phase is not a robust state based on the free energy expansion given in Eq. 1.

## VII. ACKNOWLEDGEMENTS

We gratefully acknowledge discussions with Jim Sauls and support from the NSF DMR-0244099.

- 
- <sup>1</sup> A.J. Leggett, *Rev. Mod. Phys.* **47**, 331 (1975).  
<sup>2</sup> E.V. Thuneberg, *Phys. Rev. B* **36**, 3583 (1987); E.V. Thuneberg, *J. Low Temp. Phys.* **122**, 657 (2001).  
<sup>3</sup> J.A. Sauls and J.W. Serene, *Phys. Rev. B* **24**, 183 (1981).  
<sup>4</sup> D. Rainer and J.W. Serene, *Phys. Rev. B* **13**, 4745 (1976).  
<sup>5</sup> T.M. Haard, Ph.D. thesis, Northwestern University, 2001, (unpublished).  
<sup>6</sup> J.B. Kycia *et al.* *Phys. Rev. Lett.* **72**, 864 (1994).  
<sup>7</sup> J.B. Kycia, Ph.D. thesis, Northwestern University, 1997, (unpublished).  
<sup>8</sup> D. Volhardt and P. Wölfle, *The Superfluid Phases of Helium 3*, Taylor and Francis, (1990)  
<sup>9</sup> K. Levin and O.T. Valls, *Phys. Rev. B* **20**, 105 (1979); *ibid* **20**, 120 (1979).  
<sup>10</sup> D.S. Greywall, *Phys. Rev. B* **33**, 7520 (1986).  
<sup>11</sup> M.R. Rand *et al.*, *Physica B* **194-196**, 805 (1994).  
<sup>12</sup> M.R. Rand, Ph.D. thesis, Northwestern University, (unpublished) (1996).  
<sup>13</sup> Y.H. Tang *et al.*, *Phys. Rev. Lett.* **67**, 1775 (1991).  
<sup>14</sup> U.E. Israelsson *et al.*, *Phys. Rev. Lett.* **53**, 1943 (1984).  
<sup>15</sup> E.V. Thuneberg, *Phys. Rev. B* **44**, 9685 (1991).  
<sup>16</sup> D.D. Osheroff and M.C. Cross, *Phys. Rev. Lett.* **38**, 905 (1977).  
<sup>17</sup> M. Bartkowiak *et al.*, *Phys. Rev. Lett.* **93**, 045301 (2004).  
<sup>18</sup> L.R. Corrucini and D.D. Osheroff, *Phys. Rev. Lett.* **34**, 695 (1974).  
<sup>19</sup> A.I. Ahonen *et al.*, *Phys. Lett.* **51A**, 279 (1975).  
<sup>20</sup> A.I. Ahonen, M. Krusius, and M.A. Paalanen, *J. Low Temp. Phys.* **25**, 421 (1976).  
<sup>21</sup> R.F. Hoyt, H.N. Scholz, and D.O. Edwards, *Physica* **107B**, 287 (1981).  
<sup>22</sup> D.N. Paulson, R.T. Johnson, and J.C. Wheatley, *Phys. Rev. Lett.* **31**, 746 (1973).  
<sup>23</sup> D.N. Paulson, H. Kojima, and J.C. Wheatley, *Phys. Rev. Lett.* **32**, 1098 (1974).  
<sup>24</sup> D.D. Osheroff, *Phys. Rev. Lett.* **33**, 1009 (1974).  
<sup>25</sup> I. Hahn *et al.*, *J. Low Temp. Phys.* **101**, 781 (1995).  
<sup>26</sup> R.A. Webb, *Phys. Rev. Lett.* **38**, 1151 (1977).  
<sup>27</sup> R.E. Sager *et al.*, *J. Low Temp. Phys.* **31**, 409 (1977).  
<sup>28</sup> I. Hahn *et al.*, *Phys. Rev. Lett.* **81**, 618 (1998).  
<sup>29</sup> H.N. Scholz, Ph.D. thesis, The Ohio State University, 1981, (unpublished).  
<sup>30</sup> G.F. Moores, Ph.D. thesis, Northwestern University, 1993, (unpublished).  
<sup>31</sup> N.A. Greaves, *J. Phys. C* **9**, L181 (1976).  
<sup>32</sup> C.M. Gould, *Physica B* **178**, 266 (1992).  
<sup>33</sup> T.R. Mullins *et al.*, *Phys. Rev. Lett.* **72**, 4117 (1994).  
<sup>34</sup> E.V. Thuneberg *et al.*, *Phys. Rev. Lett.* **80**, 2861 (1998).  
<sup>35</sup> R. Hänninen and E.V. Thuneberg, *Phys. Rev. B* **67**, 214507 (2003).  
<sup>36</sup> J.A. Sauls and P. Sharma, *Phys. Rev. B* **68**, 224502 (2003).  
<sup>37</sup> W.P. Halperin and J.A. Sauls, cond-mat/0408593.  
<sup>38</sup> K. Matsumoto *et al.*, *Phys. Rev. Lett.* **79**, 253 (1997).  
<sup>39</sup> B.I. Barker *et al.*, *Phys. Rev. Lett.* **85**, 2148 (2000).  
<sup>40</sup> G. Gervais *et al.*, *Phys. Rev. B* **66**, 054528 (2002).  
<sup>41</sup> E. Nazaretski *et al.*, *J. Low Temp. Phys.* **134**, 763 (2004).  
<sup>42</sup> D.T. Sprague *et al.*, *Phys. Rev. Lett.* **75**, 661 (1995).  
<sup>43</sup> G. E. Volovik, *Pis'ma Zh. Éksp. Teor. Fiz.* **63**, 281 (1996) [*JETP Lett.* **63**, 301 (1996)].  
<sup>44</sup> Y. Imry and S. Ma, *Phys. Rev. Lett.*, **35**, 1399 (1975).  
<sup>45</sup> I.A. Fomin, *J. Low Temp. Phys.* **134**, 769 (2004).  
<sup>46</sup> O. Ishikawa *et al.*, *AIP Conf. Proc.*, **850**, 235 (2006).  
<sup>47</sup> D. D. Osheroff, private communication.  
<sup>48</sup> H.C. Choi *et al.*, *Phys. Rev. Lett.* **93**, 145302 (2004).  
<sup>49</sup> V.V. Dmitriev *et al.*, *Pis'ma ZhETF* **84**, 539 (2006).